# Phononic Resonant Relaxation in Magnetic Hysteresis of Single-Molecule Magnets

Lei Gu[1*], Jia Luo[1], Qiancheng Luo[2], Yuanqi Zhai[2], Yan-Zhen Zheng[2*], and Guoping Zhao[1,3*]

[1]*College of Physics and Electronic Engineering, Sichuan Normal University, Chengdu 610068, China*
[2]*Frontier Institute of Science and Technology (FIST), Xi'an Jiaotong University, Xi'an 710054, China*
[3]*Center for Magnetism and Spintronics, Sichuan Normal University, Chengdu 610068, China*

(Received 13 December 2024; accepted manuscript online 15 January 2025)

Lanthanide-based single-molecule magnets exhibit broad magnetic hysteresis, which manifests as slow magnetic relaxation in strong magnetic fields. However, the origin of the nontrivial hysteresis behaviors remains debated. Here, we propose two influential mechanisms: activation of optical-phonon-mediated direct transitions within the ground-state doublet and the resonant Raman process. These discoveries, coupled with the $g$-factor anisotropy, account for the observed hysteresis behaviors in the regimes of fast magnetic relaxation. Our findings complement the recognized mechanisms used to interpret the magnetic hysteresis of single-molecule magnets.

DOI: 10.1088/0256-307X/42/2/027401 CSTR: 32039.14.0256-307X.42.2.027401

*1. Introduction.* Single-molecule magnets (SMMs) have attracted significant interest in recent decades because of their potential applications in information technology.[1–6] In particular, lanthanide-based SMMs have become a major focus[7–31] owing to their large magnetic moments and strong magnetic anisotropy, which usually result in slow magnetic relaxation at high magnetic fields and temperatures. Substantial efforts have been devoted to understanding the slow magnetic relaxation of SMMs,[32–45] since the ability to maintain magnetization underpins their functionality. Despite being paramagnetic, the magnetic hysteresis of SMMs can be measured when the magnetic relaxation is slower than the sweep rate of the scanning field. Thus, magnetic hysteresis is a useful characteristic of the magnetic properties of SMMs, particularly in studies on their slow magnetic relaxation in strong magnetic fields.

Although the profiles of the magnetic hysteresis loops of SMMs approximately resemble those of ferromagnetic materials, the underlying mechanisms are distinct. In ordinary ferromagnetic materials, rapid magnetization reversal typically occurs when the magnetic field exceeds a threshold that overcomes the anisotropic barrier. However, this is not the case in lanthanide-based SMMs, because the strong magnetic anisotropy produces a barrier far beyond the experimental value. Certain mechanisms significantly accelerate magnetic relaxation in relatively low magnetic fields. Resonant quantum tunneling owing to magnetic-field-induced level crossing can significantly enhance the relaxation.[46–54] However, the magnetic field strength required to induce the crossing of the ground and first excited states was significantly higher than the experimental value. Therefore, fast magnetization reversal in lanthanide SMMs is not associated with level crossing, and the spin-state configuration appears to be featureless.

Furthermore, a magnetization drop typically occurs around the zero-field strength $H = 0$ in the magnetic hysteresis loops of the SMMs. This is generally attributed to hyperfine interactions with the nuclear spins,[55–57] which can interchange the angular momentum between the electrons and nuclear spins. However, the zero-field step persists in the samples enriched with $^{164}$Dy,[22] which have no nuclear spins. Another possible zero-field tunneling mechanism is the Landau–Zener tunneling effect,[58–62] where the spin polarization can be stochastically reversed. However, we note that both hyperfine interaction-induced tunneling and Landau-Zener tunneling are temperature insensitive, whereas resonant magnetic relaxation exhibits clear temperature dependence.[59] It is likely that a mechanism rooted in spin-phonon coupling is involved.

In the canonical understanding of magnetic relaxation in SMMs, spin-phonon interactions[63–69] play a dominant role at relatively high temperatures, whereas quantum tunneling induced by hyperfine interactions dominates at very low temperatures and in the absence of magnetic fields. It was considered that acoustic phonons are more important than optical phonons, because their low energy leads to a higher phonon population. However, optical phonons are receiving increasing attention[44,45,70] because typical SMMs are molecular crystals comprising large molecules, where the intramolecular bonds are significantly stronger than intermolecular interactions. These features imply that the inner mechanics of the molecules are weakly coupled to the lattice dynamics, and that optical phonons may play a major role in magnetic relaxation, a view supported by experimental studies[64,71–73] and *ab initio*

*Corresponding author. Email: gulei@sicnu.edu.cn; zheng.yanzhen@xjtu.edu.cn; zhaogp@uestc.edu.cn
© 2025 Chinese Physical Society and IOP Publishing Ltd. All rights, including for text and data mining, AI training, and similar technologies, are reserved.

calculations.[74]

Here, we propose optical phonon-mediated direct transitions between ground-state doublets as the cause of fast magnetization reversal. We numerically simulated magnetic hysteresis based on a model with representative parameters, which justified the viability of the mechanism by showing that activation of this relaxation pathway may significantly enhance relaxation. The critical field strength for activation can be determined from a concise formulation, and the value is shown to be consistent with experimental observations. When the splitting between the ground-state doublets is small, the two phonon modes involved in the Raman process are located at the same peak in the phonon density of state (DOS), making the Raman relaxation strong. This resonant effect provides an alternative mechanism for the magnetization drop around zero field.

*2. Magneto-Modulation of the Magnetic Relaxation.* The theoretical model and parameters generally followed those described in Refs. [8,75], which describes a lanthanide-based SMM with a block temperature near the liquid nitrogen temperature. This high block temperature was largely due to the combination of strong axial magnetic anisotropy and large magnetic moments that setup a high energy barrier for the Orbach process. However, because hysteresis is observed in the temperature range of the Raman regime and the mechanisms investigated here are pronounced at low temperatures, the temperature is set to $T = 2\,\mathrm{K}$, unless noted otherwise. Furthermore, because these mechanisms are related to optical phonons, we exclusively modeled magnetic relaxation mediated by coupling with optical phonons.

The spin-phonon coupling of optical phonons takes the following form:[75]

$$\boldsymbol{H}_{\mathrm{sp}}^{\mathrm{o}} = \zeta_{\mathrm{o}} \sum_{k,q} \sum_{\Gamma} \frac{1}{\sqrt{\omega_\Gamma}} \frac{\partial B_k^q}{\partial u_\Gamma} (a_\Gamma^\dagger + a_\Gamma) O_k^q, \tag{1}$$

where $\zeta_{\mathrm{o}}$ is a tunable factor, $O_k^q$ denotes the Stevens operators, $B_k^q$ represents the crystal field parameters, $\Gamma$ indicates the phonon modes, and $u_\Gamma$ denotes the displacement along the mode. For simplicity and genericness, we assume that the DOS of optical phonons results from the level broadening of the vibrational mode with equally spaced energies [inset of Fig. 1(b)] and the invariant spin-phonon coupling strength.

We first investigated the magnetic hysteresis of a single crystal with a magnetic field along the magnetic easy axis; the magnetic hysteresis loop is presented in Fig. 1(a). The slow magnetic relaxation in weak fields corresponds to the Raman relaxation processes, as shown in the upper-left inset. The Raman process between the ground-state doublet involves a virtual transition to an excited spin state by simultaneously absorbing a phonon and emitting another. Consequently, the corresponding relaxation rate was determined by the product of the DOS of the two phonons. Energy conservation implies that the energy difference between the two phonons is equal to the energy splitting between the ground-state doublets. When the splitting matches the energy difference between the two DOS peaks, both phonons can be located at the DOS peak, and the relaxation rate reaches its maximum. To highlight the variation caused by the direct processes, a varying small coupling $\zeta_{\mathrm{o}}$ was used. The Raman relaxation is so slow that the variation in the relaxation rate within the Raman regime is almost invisible.

As the strength of the magnetic field increases, the Zeeman splitting between the ground-state doublets is enhanced. When the splitting reaches the energy range of the distribution of optical phonon modes, the direct transitions (shown in the lower right inset) between the ground-state doublets become prominent, and the magnetic relaxation is significantly enhanced. The kicks in the magnetization reversal region indicate a significant magnetic relaxation that occurs when the energy splitting matches the peak energies of the phonon DOS. Figure 1(b) presents the underlying relaxation rates of the hysteresis loops. In accordance with the loop curve, the relaxation rate increased by 3–5 orders when the direct transitions were switched on. The fluctuations in this regime correspond directly to the peaks and valleys of the phonon DOSs.

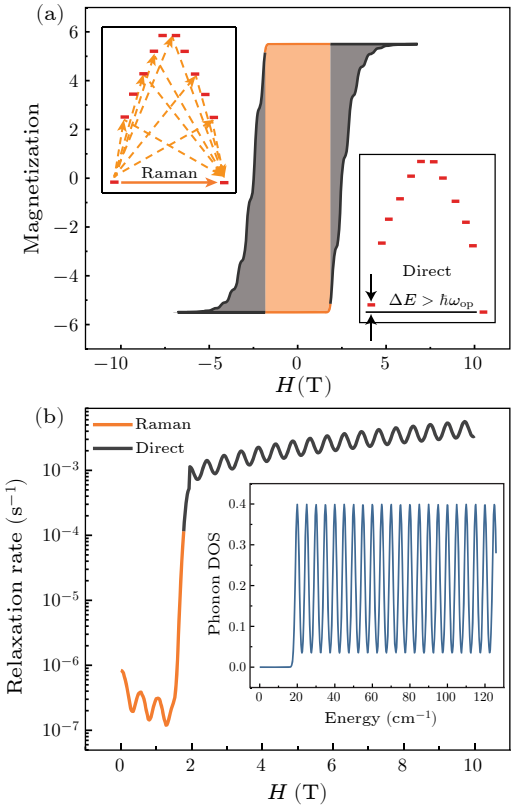


**Fig. 1.** (a) When the magnetic fields reach a critical strength, the magnetization is reversed rapidly. The rate leap around $H = 2.0\,\mathrm{T}$ in (b) is the direct cause for the rapid magnetic reversal. (b) The rate leap indicates switch-on of direct transition between the ground state doublet; the rate peaks in the direct transition regime, the phonon DOS peaks, and the sharpening in the magnetization reversal region correspond to each other. The phonon DOS results from Gaussian broadening of discrete modes with step $5\,\mathrm{cm}^{-1}$, and the width is $1\,\mathrm{cm}^{-1}$.

*3. Role of High g-Factor Anisotropy.* To activate the direct transition between the ground state doublets, the Zeeman splitting must reach the energy range associated with optical phonons. Denoting the starting frequency of the optical phonon spectrum by $\omega_{\rm op}$, the critical field strength is given by $H_{\rm c} \approx \hbar\omega_{\rm op}/2S\mu_{\rm B}g$. However, the activation process proceeds gradually when the specimen is a polycrystal and the $g$-factor is anisotropic. For instance, dysprosium complexes generally have a $g$-factor biased toward the magnetic easy axis, and the two transverse components are close to zero. In a coordinate system in which the $z$-axis is aligned with the easy axis, the $g$-factor takes the form shown in Fig. 2(a). Consequently, projection $H_z$ determines the magnitude of the Zeeman splitting. For a magnetic field of strength $H$, direct transition is activated in molecules with easy axes within the solid angle, as denoted by the red crown in Fig. 2(a). Therefore, in polycrystals, or equivalently, specimens in the form of powder, gel, or solution, $H_{\rm c}$ is the critical field strength at which the acceleration of the magnetization reversal begins, and the $g$-factor anisotropy smoothens the overall reversal and broadens the hysteresis loops, as shown in Fig. 2(b). Note that $H_{\rm c}$ does not directly determine the observed coercive field, which also depends on the orientation distribution of the molecules, relaxation time, and sweep rate of the scanning field.

Because of the $g$-factor anisotropy and tilted easy axes, direct transition in most molecules was activated only when the magnetic field was considerably stronger than $H_{\rm c}$. The overall magnetic relaxation above the critical field strength was significantly slower than that in the single-crystal, because a considerable portion of the molecules continued to undergo slow Raman relaxation. As a result, magnetic hysteresis can still be observed, even for much stronger spin-phonon coupling. The coupling strength for the wider loop is $\zeta_{\rm o} = 12\,\text{Å/s}^{-1}$, whereas that for the narrower loop [Fig. 1(a)] is $\zeta_{\rm o} = 0.6\,\text{Å/s}^{-1}$. Under strong spin–phonon coupling, a visible magnetization reduction occurs near $H = 0\,\text{T}$. At $H = 0\,\text{T}$, the Zeeman splitting is zero, and every molecule undergoes resonant Raman relaxation regardless of the direction of the easy axis. The resonant Raman relaxations at wider splitting are not obvious in the hysteresis loop because at a certain magnetic field away from $H = 0\,\text{T}$, such resonances occur only in a limited number of molecules. For a similar reason, the drastic magnetization reversal became less sharp.

*4. Experimental Relevance.* Figure 2(c) presents the magnetic hysteresis loops of the $[\text{Dy(1-AdO)}_2(\text{py})_5]\text{BPh}_4$ complex in solution. The lowest phonon energy and axial $g$-value were calculated as $\hbar\omega \approx 1.2\,\text{meV}$ and $g_z = 1.3$, respectively (see the SM). With $S = 15/2$, we obtain $H_{\rm c} \approx 0.8\,\text{T}$, which agrees well with the experimental values. Remarkably, two modes with energies of approximately $3.2\,\text{meV}$ ($26\,\text{cm}^{-1}$) in the calculated vibration spectrum (see the SM) account for the sharp drop close to $H = 2\,\text{T}$. This further corroborates our proposed mechanism and suggests that the resonant relaxation may provide a means of measuring the energies of the lowest optical phonons.

The proposed coercivity mechanism is further supported by several other studies, in which the acceleration of relaxation at similar field strengths is commonly observed in magnetic hysteresis measurements of SMMs.[7–31] Moreover, given that experimental and computational data are available, we find that the consistency is quantitative. For example, in Ref. [10] the lowest phonon energy is approximately twice the value reported here, and the observed $H_{\rm c}$ doubles.

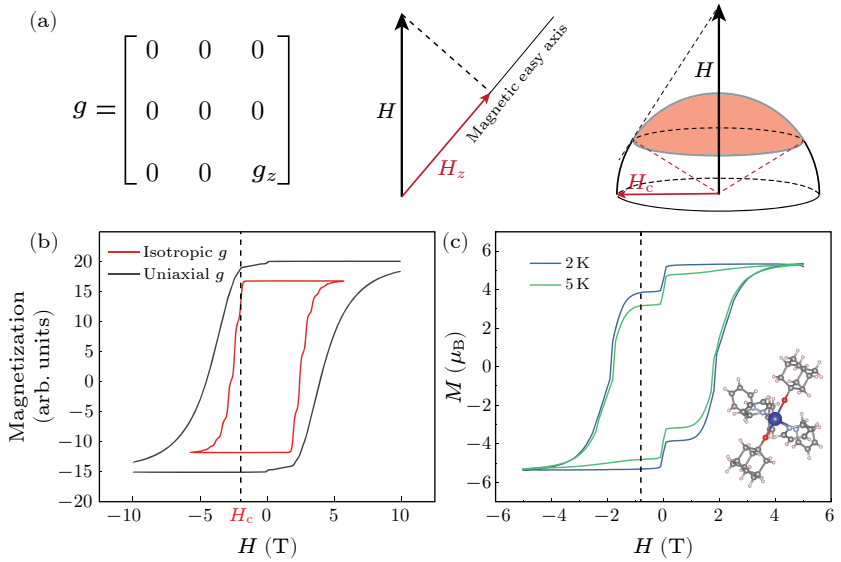


**Fig. 2.** (a) For molecules whose $g$-factor is completely biased to the easy axis, projection of magnetic field onto the axis essentially causes Zeeman splitting. Given a magnetic field, direct transition is activated if the easy axis of the magnetic moment is within the solid angle denoted by the red crown. (b) Anisotropy of the molecular $g$-factor smoothens the activation process in polycrystalline specimens and broadens the hysteresis loops. (c) The measured magnetic hysteresis loops for the $[\text{Dy(1-AdO)}_2(\text{py})_5]\text{BPh}_4$ are complex. The critical field strength $H_{\rm c}$ (marked by the dashed line) agrees with the theoretical prediction.

According to this picture, a decisive factor for magnetic hysteresis is the increase in the relaxation rate once the direct transition between the ground doublets is activated. The large magnitude of the magnetic moment plays a dual role: it facilitates strong axiality but reduces the critical field strength. However, hardening of the low-energy vibrational modes directly increases the critical field strength. In addition, for specimens in the form of polycrystals, powders, gels, or solutions, the anisotropy of the $g$-factor delays the activation of the direct transition of molecules with tilted easy axes. This effect smoothens the magnetization drops, broadens the hysteresis loop, and enables the observation of magnetic hysteresis for significantly stronger spin–phonon coupling than in the single-crystal case.

However, a large magnetic moment with strong axial anisotropy is the most common strategy for achieving slow magnetic relaxation of SMMs;[76–80] hence, magnetic hysteresis can be observed. This suppresses direct transitions, such that Raman processes can dominate at relatively high temperatures. The advantage of rare-earth SMMs is the weak covalent involvement of local f-electrons,[81] which curbs the impact of molecular vibrations. The strategic design of molecules with symmetry considerations can weaken the phonon coupling and reduce the relaxation rate.[80,82] Moreover, the symmetry strategy and intramolecular exchange interactions can be leveraged to reduce quantum tunneling.[78]

In many hysteresis measurements, the magnetic relaxation in the weak-field regime is not sufficiently slow to maintain magnetization, and the magnetization is either diminished to nearly zero or reversed before the critical field is reached. In such cases, the optical-phonon-mediated direct process does not affect magnetization reversal, but results in accelerated magnetization toward saturation (see for example, Refs. [24–26,83]). In some magnetic molecules, most commonly those containing nitrogen in the ligand, hyperfine interactions can cause transitions between the ground-state doublets by exchanging angular momentum between the nuclei and electrons. As the nuclear spin states are nearly degenerate, energy conservation implies that this relaxation process occurs when the Zeeman splitting is close to zero.

Nevertheless, we argue that hyperfine interaction-induced relaxation is ineffective or only plays a minor role in dysprosocenium and other molecules with large spins. Among the stable isotopes of dysprosium, $^{161}$Dy and $^{163}$Dy can undergo such relaxation because their isospins are not zero, but $I = 5/2$. However, to mediate the flipping of an electron's angular momentum of $S = 15/2$, hyperfine interaction-induced tunneling can only be effective up to the third order. This implies that the effect could be significantly smaller in dysprosocenium single-molecule magnets than in those with a smaller $S$. Direct evidence against hyperfine interaction is the observation of the zero-field step in $^{164}$ Dy-enriched samples[22] because $^{164}$Dy has no nuclear spin. However, as shown below, resonant Raman relaxation can yield significant magnetization reduction and induce a butterfly shaped magnetic hysteresis (see Refs. [24–26,83]).

A comment on the temperature dependence of the magnetization drop around the zero field is required. Hyperfine interaction-induced tunneling and Landau-Zener tunneling are temperature-insensitive. The direct process via spin–phonon coupling exhibits temperature dependence $\tau^{-1} \propto T$, but is forbidden at zero field by time-reversal symmetry. As shown in the SM, although a finite magnetic field breaks the time-reversal symmetry and enables a direct process, it remains very weak around the zero field. Therefore, it is likely that the Raman process dominates the low-field magnetic relaxation, and temperature dependence is a favorable property that justifies the presence of Raman resonance relaxation.

However, it should be noted that the temperature dependence was significant compared to the experimental trends. As indicated by the slope of the hysteresis loops in Fig. 2(c), the relaxation rate did not change significantly from $T = 2$ to $T = 5$ K. This slowly varying trend has been widely observed in other magnetic hysteresis and direct measurements of the temperature dependence of the magnetic relaxation rate.[7–31] Figure 3(b) shows the temperature dependence of the magnetic relation rate in several magnetic fields, where the rate increases by 2–4 orders as the temperature increases from 2 K to 5 K. Accordingly, the coercive field at $T = 5$ K in Fig. 3(a) is close to zero.

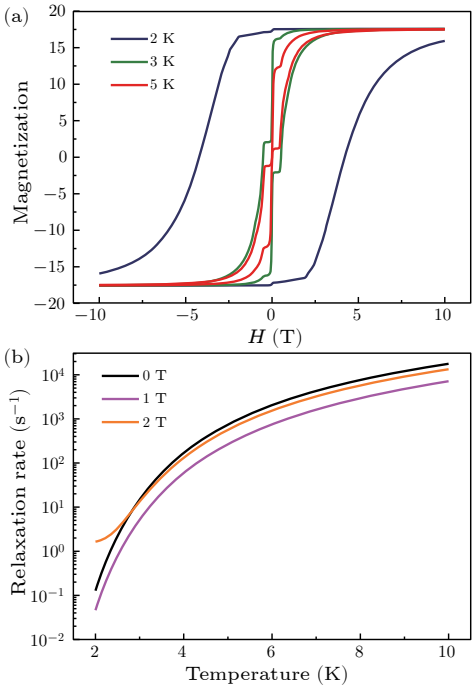


**Fig. 3.** (a) Magnetic hysteresis loops at three temperatures under optical-phonon-dominated relaxation. The fierce relaxation enhancement due to temperature rise diminishes the coercive field to small values even at $T = 3$ K. (b) Temperature dependence of the relaxation rate for typical magnetic fields; the rates are generally increased by 3 orders.

The mild temperature dependence observed in this experiment may be a procedural consequence. For lan-

thanide single-molecule magnets with slow magnetic relaxation, the relaxation time at low temperatures can be hundreds of minutes. However, the hold time for the sample to reach a stable state after temperature variations is generally several tens of minutes. It is possible that thermal equilibrium was not established before the property measurements were performed. In other words, the actual temperature of the sample may not be the recorded temperature, and the results may depend on how the sample was processed. This could be the reason for the high uncertainty in the low-temperature relaxation rate, which can differ by more than two orders of magnitude.[84] Another possibility is the phonon bottleneck effect,[85,86] in which the timescale of phonon thermalization is larger than that of the phonon-mediated processes in question. Indeed, the phonon bottleneck effect can lead to a mild temperature dependence, such as $\tau^{-1} \propto T^2$.[87] We plan to present a systematic discussion of this issue in a future study.

*5. Conclusions.* By investigating the magnetic relaxation of SMMs under magnetic fields and simulating magnetic hysteresis, we demonstrated that the resonant relaxation processes can account for the magnetization drop around zero magnetic field and the fast magnetization reversal above a critical field strength. The former occurs because the two phonons in the Raman process coincide with the same phonon DOS peak. The latter is due to the activation of the direct transition between the ground-state doublets mediated by optical phonons. When the energy splitting matches the peak energies of the phonon DOS, the magnetic relaxation becomes significant. We conclude by noting that we exclusively modeled the phononic resonance effects in this study, whereas the magnetic hysteresis behavior of SMMs is a collaborative effect that also involves other recognized or unidentified mechanisms.

*Acknowledgements.* L. G. thanks the support from the Sichuan Normal University. Q.L., Y.Z., and Y.Z. received support from the National Natural Science Foundation of China (Grant No. 22375157). G.Z. acknowledges support from the National Natural Science Foundation of China (Grant Nos. 12474122, 52171188, 51771127, and 52111530143), and the Central Government Funds of Guiding Local Scientific and Technological Development for Sichuan Province (Grant No. 2021ZYD0025).

# References

[1] Gaita-Ariño A, Luis F, Hill S, and Coronado E 2019 *Nat. Chem.* **11** 301
[2] Coronado E 2020 *Nat. Rev. Mater.* **5** 87
[3] Chilton N F 2022 *Annu. Rev. Mater. Res.* **52** 79
[4] Mirzoyan R, Kazmierczak N P, and Hadt R G 2021 *Chem. Eur. J.* **27** 9482
[5] Kazmierczak N P and Hadt R G 2022 *J. Am. Chem. Soc.* **144** 20804
[6] Yang C, Wang Z C, and Su G 2020 *Chin. Phys. Lett.* **37** 087201
[7] Wäckerlin C, Donati F, Singha A, Baltic R, Rusponi S, Diller K, Patthey F, Pivetta M, Lan Y, Klyatskaya S, Ruben M, Brune H, and Dreiser J 2016 *Adv. Mater.* **28** 5195
[8] Goodwin C A P, Ortu F, Reta D, Chilton N F, and Mills D P 2017 *Nature* **548** 439
[9] Abbasi P, Quinn K, Alexandropoulos D I, Damjanović M, Wernsdorfer W, Escuer A, Mayans J, Pilkington M, and Stamatatos T C 2017 *J. Am. Chem. Soc.* **139** 15644
[10] Guo F S, Day B M, Chen Y C, Tong M L, Mansikkamäki A, and Layfield R A 2018 *Science* **362** 1400
[11] Randall McClain K, Gould C A, Chakarawet K, Teat S J, Groshens T J, Long J R, and Harvey B G 2018 *Chem. Sci.* **9** 8492
[12] Gould C A, McClain K R, Reta D, Kragskow J G C, Marchiori D A, Lachman E, Choi E S, Analytis J G, Britt R D, Chilton N F, Harvey B G, and Long J R 2022 *Science* **375** 198
[13] Rinehart J D, Fang M, Evans W J, and Long J R 2011 *Nat. Chem.* **3** 538
[14] Rinehart J D, Fang M, Evans W J, and Long J R 2011 *J. Am. Chem. Soc.* **133** 14236
[15] Guo Y N, Xu G F, Wernsdorfer W, Ungur L, Guo Y, Tang J, Zhang H J, Chibotaru L F, and Powell A K 2011 *J. Am. Chem. Soc.* **133** 11948
[16] Demir S, Zadrozny J M, Nippe M, and Long J R 2012 *J. Am. Chem. Soc.* **134** 18546
[17] Langley S K, Wielechowski D P, Vieru V, Chilton N F, Moubaraki B, Abrahams B F, Chibotaru L F, and Murray K S 2013 *Angew. Chem. Int. Ed.* **52** 12014
[18] Chen Y C, Liu J L, Ungur L, Liu J, Li Q W, Wang L F, Ni Z P, Chibotaru L F, Chen X M, and Tong M L 2016 *J. Am. Chem. Soc.* **138** 2829
[19] Demir S, Gonzalez M I, Darago L E, Evans W J, and Long J R 2017 *Nat. Commun.* **8** 2144
[20] Ding Y S, Yu K X, Reta D, Ortu F, Winpenny R E P, Zheng Y Z, and Chilton N F 2018 *Nat. Commun.* **9** 3134
[21] Liu F, Krylov D S, Spree L, Avdoshenko S M, Samoylova N A, Rosenkranz M, Kostanyan A, Greber T, Wolter A U B, Büchner B, and Popov A A 2017 *Nat. Commun.* **8** 16098
[22] Ortu F, Reta D, Ding Y S, Goodwin C A P, Gregson M P, McInnes E J L, Winpenny R E P, Zheng Y Z, Liddle S T, Mills D P, and Chilton N F 2019 *Dalton Trans.* **48** 8541
[23] Yu K X, Kragskow J G C, Ding Y S, Zhai Y Q, Reta D, Chilton N F, and Zheng Y Z 2020 *Chem* **6** 1777
[24] Huang W, Shen F X, Wu S Q, Liu L, Wu D, Zheng Z, Xu J, Zhang M, Huang X C, Jiang J, Pan F, Li Y, Zhu K, and Sato O 2016 *Inorg. Chem.* **55** 5476
[25] Santana F S, Perfetti M, Briganti M, Sacco F, Poneti G, Ravera E, Soares J F, and Sessoli R 2022 *Chem. Sci.* **13** 5860
[26] Zabala-Lekuona A, Seco J M, and Colacio E 2021 *Coord. Chem. Rev.* **441** 213984
[27] Chen C H, Spree L, Koutsouflakis E, Krylov D S, Liu F P, Brandenburg A, Velkos G, Schimmel S, Avdoshenko S M, Fedorov A, Weschke E, Choueikani F, Ohresser P, Dreiser J, Büchner B, and Popov A A 2021 *Adv. Sci.* **8** 2000777
[28] Ding X L, Luo Q C, Zhai Y Q, Zhang X F, Lv Y, Zhang X L, Ke C, Wu C, and Zheng Y Z 2022 *Chin. J. Chem.* **40** 563
[29] Guo F S, He M, Huang G Z, Giblin S R, Billington D, Heinemann F W, Tong M L, Mansikkamäki A, and Layfield R A 2022 *Inorg. Chem.* **61** 6017
[30] Ling B K, Zhai Y Q, Jin P B, Ding H F, Zhang X F, Lv Y, Fu Z, Deng J, Schulze M, Wernsdorfer W, and Zheng Y Z 2022 *Matter* **5** 3485
[31] Chen Q W, Ding Y S, Xue T, Zhu X F, and Zheng Z 2023 *Inorg. Chem. Front.* **10** 6236
[32] Harman W H, Harris T D, Freedman D E, Fong H, Chang A, Rinehart J D, Ozarowski A, Sougrati M T, Grandjean F, Long G J, Long J R, and Chang C J 2010 *J. Am. Chem. Soc.* **132** 18115

[33] Vallejo J, Castro I, Ruiz-García R, Cano J, Julve M, Lloret F, De Munno G, Wernsdorfer W, and Pardo E 2012 *J. Am. Chem. Soc.* **134** 15704

[34] Zhu Y Y, Cui C, Zhang Y Q, Jia J H, Guo X, Gao C, Qian K, Jiang S D, Wang B W, Wang Z M, and Gao S 2013 *Chem. Sci.* **4** 1802

[35] Zadrozny J M, Atanasov M, Bryan A M, Lin C Y, Rekken B D, Power P P, Neese F, and Long J R 2013 *Chem. Sci.* **4** 125

[36] Lucaccini E, Sorace L, Perfetti M, Costes J P, and Sessoli R 2014 *Chem. Commun.* **50** 1648

[37] Gómez-Coca S, Urtizberea A, Cremades E, Alonso P J, Camón A, Ruiz E and Luis F 2014 *Nat. Commun.* **5** 4300

[38] Liddle S T and van Slageren J 2015 *Chem. Soc. Rev.* **44** 6655

[39] Rajnák C, Titiš J, Moncoľ J, Renz F, and Boča R 2019 *Chem. Commun.* **55** 13868

[40] Wang J, Ruan Z Y, Li Q W, Chen Y C, Huang G Z, Liu J L, Reta D, Chilton N F, Wang Z X, and Tong M L 2019 *Dalton Trans.* **48** 1686

[41] Kobayashi F, Ohtani R, Nakamura M, Lindoy L F, and Hayami S 2019 *Inorg. Chem.* **58** 7409

[42] Cui H H, Lu F, Chen X T, Zhang Y Q, Tong W, and Xue Z L 2019 *Inorg. Chem.* **58** 12555

[43] Vallejo J, Viciano-Chumillas M, Lloret F, Julve M, Castro I, Krzystek J, Ozerov M, Armentano D, De Munno G, and Cano J 2019 *Inorg. Chem.* **58** 15726

[44] Gu L and Wu R 2020 *Phys. Rev. Lett.* **125** 117203

[45] Kragskow J G C, Mattioni A, Staab J K, Reta D, Skelton J M, and Chilton N F 2023 *Chem. Soc. Rev.* **52** 4567

[46] Thomas L, Lionti F, Ballou R, Gatteschi D, Sessoli R, and Barbara B 1996 *Nature* **383** 145

[47] Friedman J R, Sarachik M P, Tejada J, and Ziolo R 1996 *Phys. Rev. Lett.* **76** 3830

[48] Hernández J M, Zhang X X, Luis F, Bartolomé J, Tejada J, and Ziolo R 1996 *Europhys. Lett.* **35** 301

[49] Barbara B, Thomas L, Lionti F, Sulpice A, and Caneschi A 1998 *J. Magn. Magn. Mater.* **177** 1324

[50] Kent A D, Zhong Y, Bokacheva L, Ruiz D, Hendrickson D N, and Sarachik M P 2000 *J. Appl. Phys.* **87** 5493

[51] Kent A D, Zhong Y, Bokacheva L, Ruiz D, Hendrickson D N, and Sarachik M P 2000 *Europhys. Lett.* **49** 521

[52] Zhong Y, Sarachik M P, Yoo J, and Hendrickson D N 2000 *Phys. Rev. B* **62** R9256

[53] Chiorescu I, Giraud R, Jansen A G M, Caneschi A, and Barbara B 2000 *Phys. Rev. Lett.* **85** 4807

[54] Gatteschi D and Sessoli R 2003 *Angew. Chem. Int. Ed.* **42** 268

[55] Giraud R, Wernsdorfer W, Tkachuk A M, Mailly D, and Barbara B 2001 *Phys. Rev. Lett.* **87** 057203

[56] Ishikawa N, Sugita M, and Wernsdorfer W 2005 *J. Am. Chem. Soc.* **127** 3650

[57] Chen Y C, Liu J L, Wernsdorfer W, Liu D, Chibotaru L F, Chen X M, and Tong M L 2017 *Angew. Chem. Int. Ed.* **56** 4996

[58] Rousochatzakis I, Ajiro Y, Mitamura H, Kögerler P, and Luban M 2005 *Phys. Rev. Lett.* **94** 147204

[59] Wernsdorfer W, Bhaduri S, Vinslava A, and Christou G 2005 *Phys. Rev. B* **72** 214429

[60] Vogelsberger M and Garanin D A 2006 *Phys. Rev. B* **73** 092412

[61] Irländer K and Schnack J 2020 *Phys. Rev. B* **102** 054407

[62] Mattioni A, Staab J K, Blackmore W J A, Reta D, Iles-Smith J, Nazir A, and Chilton N F 2024 *Nat. Commun.* **15** 2041

[63] Shrivastava K N 1983 *Phys. Status Solidi* **117** 437

[64] Briganti M, Santanni F, Tesi L, Totti F, Sessoli R, and Lunghi A 2021 *J. Am. Chem. Soc.* **143** 13633

[65] Reta D, Kragskow J G C, and Chilton N F 2021 *J. Am. Chem. Soc.* **143** 5943

[66] Gu L, Li J, and Wu R 2022 *J. Magn. Magn. Mater.* **564** 170138

[67] Lunghi A 2022 *Science Advances* **8** eabn7880

[68] Lunghi A 2023 *Spin-phonon relaxation in magnetic molecules: Theory, predictions and insights Challenges and Advances in Computational Chemistry and Physics* (Springer International Publishing) p. 219

[69] Su D, Zhang Y Q, Liu E K, and Sun Y 2023 *Chin. Phys. B* **32** 087505

[70] Gu L and Wu R 2021 *Phys. Rev. B* **103** 014401

[71] Ma Y, Zhai Y Q, Luo Q C, Ding Y S, and Zheng Y Z 2022 *Angew. Chem.* **134** e202206022

[72] Garlatti E, Tesi L, Lunghi A, Atzori M, Voneshen D J, Santini P, Sanvito S, Guidi T, Sessoli R, and Carretta S 2020 *Nat. Commun.* **11** 1751

[73] Garlatti E, Albino A, Chicco S, Nguyen V H A, Santanni F, Paolasini L, Mazzoli C, Caciuffo R, Totti F, Santini P, Sessoli R, Lunghi A, and Carretta S 2023 *Nat. Commun.* **14** 1653

[74] Nabi R, Staab J K, Mattioni A, Kragskow J G C, Reta D, Skelton J M, and Chilton N F 2023 *J. Am. Chem. Soc.* **145** 24558

[75] Chiesa A, Cugini F, Hussain R, Macaluso E, Allodi G, Garlatti E, Giansiracusa M, Goodwin C A P, Ortu F, Reta D, Skelton J M, Guidi T, Santini P, Solzi M, De Renzi R, Mills D P, Chilton N F, and Carretta S 2020 *Phys. Rev. B* **101** 174402

[76] Li J, Yang Y, Yu Q, Su G, and Liu W 2024 *J. Phys. Chem. C* **128** 4882

[77] Li H D, Wu S G, and Tong M L 2023 *Chem. Commun.* **59** 6159

[78] Wang J, Sun C Y, Zheng Q, Wang D Q, Chen Y T, Ju J F, Sun T M, Cui Y, Ding Y, and Tang Y F 2023 *Chemistry-An Asian J.* **18** e202201297

[79] Yin X, Deng L, Ruan L, Wu Y, Luo F, Qin G, Han X, and Zhang X 2023 *Materials* **16** 1996

[80] Ashebr T G, Li H, Ying X, Li X L, Zhao C, Liu S, and Tang J 2022 *ACS Materials Lett.* **4** 307

[81] Liu M, Peng X H, Guo F S, and Tong M L 2023 *Inorg. Chem. Front.* **10** 3742

[82] Liu J L, Chen Y C, and Tong M L 2018 *Chem. Soc. Rev.* **47** 2431

[83] El Beyrouti N, Houard F, Cordier M, Trzop E, Rigaut S, Le Guennic B, Bernot K, and Norel L 2023 *Chem. Commun.* **59** 5265

[84] Blackmore W J A, Gransbury G K, Evans P, Kragskow J G C, Mills D P, and Chilton N F 2023 *Phys. Chem. Chem. Phys.* **25** 16735

[85] Gill J C 1973 *J. Phys. C: Solid State Phys.* **6** 109

[86] Garanin D A 2007 *Phys. Rev. B* **75** 094409

[87] Abragam A and Bleaney B 2012 *Electron paramagnetic resonance of transition ions* (Oxford: Oxford University Press)